Supporting Information

Re-investigation of HExxH enzyme DarF reveals a dehydrogenation-epoxidation reactions

Jabal Rahmat Haedar,[a] Nils Böhringer,[b] Gaja Swarna Kumari,[a] Vic Kiselov,[a] Viktors Romanuks,[a] Gints Smits,[ac] Stefano Donadio,[ad] Till F. Schäberle,[bef] and Chin-Soon Phan,*[a]

[a] Latvian Institute of Organic Synthesis, Aizkraukles Street 21, LV-1006 Riga, Latvia.
[b] Natural Product Research, Institute for Insect Biotechnology, Justus-Liebig-University Giessen, 35392 Gießen, Germany.
[c] Faculty of Natural Sciences and Technology, Riga Technical University, Paula Valdena 3, LV-1048, Riga, Latvia.
[d] NAICONS Srl, 20139 Milan, Italy.
[e] Fraunhofer Institute for Molecular Biology and Applied Ecology, Branch of Bioresources, Ohlebergsweg 12, 35392 Gießen, Germany.
[f] German Center for Infection Research (DZIF), Partner Site Gießen-Marburg-Langen, Ohlebergsweg 12, 35392 Gießen, Germany

*Correspondence: Chin-Soon Phan, chinsoon@osi.lv

Table of Contents

EXPERIMENTAL SECTION

General. Chemicals and reagents were purchased from either Merck or Sigma-Aldrich unless otherwise specified. Synthetic genes inserted into expression vectors were synthesized by the Twist Bioscience (https://www.twistbioscience.com/). Gene sequences used in this study are listed in Table S1. Trypsin protease was purchased from Merck. Antibiotics (kanamycin, spectinomycin and chloramphenicol) were purchased from GoldBio. *Escherichia coli* NiCo21(DE3) and DH5α strains purchased from NEB were used for protein expression and plasmid preparation, respectively. Electroporation was carried out using a Bio-Rad MicroPulser. Terrific broth (TB) was purchased from Formedium. Luria broth (LB), Miller broth and agar were purchased from Carl Roth. SDS-PAGE, 4-20% polyacrylamide gel was purchased from GenScript. Protein marker, broad multi color pre-stained protein standard for SDS-PAGE was purchased from GenScript. The *E. coli* cells were lysed using a Hielscher Ultrasonics Sonotrode S26D7 Titanium 7mm. LC-MS experiments were performed on a Waters Acquity H-class UPLC System coupled to Waters QToF SYNAPT G2-Si Mass Spectrometer.

Bioinformatic expansion of darobactin BGCs containing DarF. To retrieve putative αKG-dependent HExxH enzyme DarF sequences, Basic Local Alignment Search Tool Protein (BLASTP)[1] was performed in June 2025 on a non-redundant protein database in National Center for Biotechnology Information (NCBI) online database using DarF (WP_063364329.1)[2] from *Pseudoalteromonas luteoviolacea* as query and 1E-5 as cutoff value for search. The putative darobactin precursor peptides were manually identified from the upstream regions of DarF. This resulted 12 homologous DarF enzymes linked to putative precursor peptides (Figure S1).

Phylogenetic tree construction. The αKG-dependent enzymes in RiPP biosynthesis, PoyI (AFS60645.1),[3] DurX (WP_071962208.1),[4] CanE (KUN61407.1),[5] YhhC (WP_003708570.1),[6] SmaO (WP_141401631.1),[7] $MscH_{429\text{-}768}$ (WP_013477425.1),[8] $SjiH_{460\text{-}819}$ (WP_042453644.1),[8] $ChlH_{376\text{-}722}$ (WP_016869186.1),[8] PflC (WP_192559974.1),[9] PosC (WP_060837885.1),[9] ColD (WP_033308454.1),[10] and DarF (WP_063364329.1)[2] were used to generate a phylogenetic tree. A multi-sequence alignment of these proteins generated with Clustal Omega was used to build a phylogenetic tree at EMBL-EBI platform.[11] The C-terminal HExxH domains in MscBH, SjiBH and ChlBH are referred to as MscH, SjiH and ChlH, respectively.

Transformation of plasmids into *E. coli* NiCo21(DE3). Plasmids containing precursor and rSAM genes were obtained from Twist Bioscience and dissolved in MilliQ grade water to a final concentration of 10 ng/µL. 70 µL of *E. coli* NiCo21(DE3) electrocompetent cells were transformed in a 2 mm electroporation cuvette with either 1 µL of plasmid DNA containing the precursor gene for the precursor-only expression or 1 µL of plasmid DNA containing the precursor gene + 1 µL of plasmid DNA containing the rSAM enzyme for the coexpression of the precursor and the rSAM enzyme. The transformed cells were then grown overnight at 37 °C on LB (Miller) agar supplemented with appropriate antibiotics at a final concentration of kanamycin 30 µg/mL and/or spectinomycin 100 µg/mL.

Protein expression and purification of precursor peptides. A colony from the transformation above was picked up by a toothpick and added to 3 mL TB medium supplemented with appropriate antibiotics in a 15 mL falcon tube. The 50 mL culture was grown overnight at 37°C and shaken at 250 rpm. The overnight culture was used to inoculate either 250 mL of antibiotic-supplemented TB media in a 1 L Erlenmeyer flask in a 1:100 (v:v) ratio. The cells were then grown at 37°C, 250 rpm until $OD_{600\ nm}$ reached 1.8-2.4. The culture was then placed on ice water for 30 min and protein expression was induced by addition of IPTG at a 0.1 mM final concentration. After induction, the culture was shaken at 16°C, 250 rpm for 18 h. The cells were collected by centrifugation at 4000 rpm for 10 min. The denaturing lysis buffer (100 mM NaH_2PO_4, 10 mM Tris, 8 M Urea, 10 mM imidazole, pH 8) was added to cell pellets in a ratio of 3:1 (v:w). The cell pellets were reconstituted and lysed by sonication with a Titanium 7mm solid probe (20 sec on and 15 sec off for 25 cycles at 50% amplitude). After sonication, the cell debris was removed by centrifugation at 15,000 rpm for 15 min. HisPur Ni-NTA resin (0.7 mL) was added to ~15-20 mL of supernatant in a 50 mL falcon tube and gently shaken for 1 h to allow binding of the precursor peptide to the Ni-NTA resin. Peptide-bound Ni-NTA resin was then washed with denaturing lysis buffer (2 x 1 mL for 0.7 mL resin if this buffer was used to resuspend the cell pellet), NPI-20 (50 mM NaH_2PO_4, 300 mM NaCl, 20 mM imidazole, pH 8, 5 x 1 mL for 0.7 mL resin) and eluted with NPI-250 (50 mM NaH_2PO_4, 300 mM NaCl, 250 mM imidazole, pH 8, 2.5 mL for 0.7 mL resin). Elution fractions were desalted into 50 mM Tris buffer (pH 8.0) using PD Minitrap G-10 columns. The full-length His_6-SUMO-precursor peptide obtained by coexpression of DarA + DarE was digested with 1 mg/mL trypsin (1:100, trypsin/eluant v:v) at 37°C for 16 h and analyzed by LC-MS to detect activity from the radical SAM enzyme DarE, while the undigested full-length His_6-SUMO-precursor peptide was used as a substrate for the biochemical characterization of αKG-dependent HExxH enzyme DarF.

Protein expression and purification of HExxH enzyme DarF. A colony from the transformation above was picked up by a toothpick and added to 5 mL TB medium supplemented with appropriate antibiotics in a 15 mL falcon tube. The 50 mL culture was grown overnight at 37°C and shaken at 250 rpm. The overnight culture was used to inoculate either 250 mL of antibiotic-supplemented TB media in a 1 L Erlenmeyer flask in a 1:100 (v:v) ratio. The cells were then grown at 37°C, 250 rpm until $OD_{600\ nm}$ reached 1.8-2.4. The culture was then placed on ice water for 30 min and protein expression was induced by addition of IPTG at a 0.1 mM final concentration. After induction, the culture was shaken at 16°C, 250 rpm for 18 h. The cells were collected by centrifugation at 4000 rpm for 10 min. The non-denaturing buffer (50 mM NaH_2PO_4, 10 mM Tris, 10 mM imidazole, 300 mM NaCl, 10% glycerol, pH 8) was added to cell pellets in a ratio of 3:1 (v:w). The cell pellets were reconstituted and lysed by sonication with a Titanium 7mm solid probe (10 sec on and 15 sec off for 25 cycles at 30% amplitude). After sonication, the cell debris was removed by centrifugation at 15,000 rpm for 15 min. HisPur Ni-NTA resin (0.7 mL) was added to ~15-20 mL of supernatant in a 50 mL falcon tube and gently shaken for 1 h to allow binding of the precursor peptide to the Ni-NTA resin. Peptide-bound Ni-NTA resin was then washed with non-denaturing buffer (2 x 1 mL for 0.7 mL resin if this buffer was used to resuspend the cell pellet), NPI-20 (50 mM NaH_2PO_4, 300 mM NaCl, 20 mM imidazole, pH 8, 5 x 1 mL for 0.7 mL resin) and eluted with NPI-250 (50 mM NaH_2PO_4, 300 mM NaCl, 250 mM imidazole, pH 8, 2.5 mL for 0.7 mL resin). Elution fractions were desalted into 50 mM Tris buffer (pH 8.0) using PD Minitrap G-10 columns. Purified His_6-DarF was determined by SDS-PAGE and subjected to *in vitro* assay.

LC-MS conditions. Data acquisition was performed using MestReNova at the following conditions.

Waters UPLC system Acquity H-class connected with Waters UV detector PDA eλ coupled with Waters TOF mass spectrometer SYNAPT G2-Si.

LC: column = Acquity BEH C18, 1.7 μm, 2.1 x 50 mm; mobile phase/gradient = solvent A: H_2O + 0.1 % formic acid, solvent B: CH_3CN, Initial – 95 % A, 1.5 min – 40 % A, 2.5 min – 2 % A, 3.5 min – 2 % A, 3.7 min – 95 % A, 6 min – 95 % A; flow rate = 0.4 mL/min; column temp. = 40 °C; Injection volume = 1 μL, Run time = 6 min

MS: polarity = positive; capillary voltage = +0.7 kV; cone voltage = 40.0 V; source temperature = 120 °C; desolvation temperature = 500 °C; cone gas flow = 30 L/h; desolvation gas flow = 800 L/h; collision energy = 4 V; mass range = *m/z* 250–2000; scan duration = 0.5 s; interscan delay = 0.025 s; data acquisition = continuum mode; Lockspray (Leucine enkephalin); scan duration = 1.0 s; interval = 10 scans.

MS/MS: polarity = positive; scan duration = 1.0 s; inter-scan delay = 0.025 s; data acquisition = continuum mode; mass range and collision energy are specified in the respective figure legends.

***In vitro* assay of DarF**. His_6-DarF biochemical characterization was carried out in 50 mM Tris-HCl buffer (pH 8.0) with purified DarE modified full-length His_6-precursor peptide (0.1 - 0.2 mM), 0.5 mM of $Fe(SO_4)_2(NH_4)_2$, 2 mM of αKG, 2 mM of ascorbate and 10 μM of enzyme His_6-DarF in a reaction volume of 100 μL. For the negative control, enzyme His_6-DarF was boiled by heating at 80 °C for 10 min. The reaction solution was incubated at 28 °C for 2 h and quenched with absolute methanol. After centrifugation at 15,000 rpm for 10 min, the products were then subjected to LC-MS analysis as mentioned above.

Time-course *in vitro* assay of DarF. His_6-DarF biochemical characterization was carried out in 50 mM Tris-HCl buffer (pH 8.0) with purified DarE modified full-length His_6-precursor peptide (50 μM), 0.5 mM of $Fe(SO_4)_2(NH_4)_2$, 2 mM of αKG, 2 mM of ascorbate and 1 μM of enzyme His_6-DarF in a reaction volume of 1 mL. The reaction solution was incubated at 28 °C for 0, 1, 5, 30 and 60 min, then quenched with absolute methanol. After centrifugation at 15,000 rpm for 10 min, the products were then subjected to LC-MS analysis as mentioned above.

Enzyme concentration-dependent *in vitro* assay of DarF. His_6-DarF biochemical characterization was carried out in 50 mM Tris-HCl buffer (pH 8.0) with purified DarE modified full-length His_6-precursor peptide (50 μM), 0.5 mM of $Fe(SO_4)_2(NH_4)_2$, 2 mM of αKG, 2 mM of ascorbate and 1, 5, 10 and 20 μM of enzyme His_6-DarF in a reaction volume of 150 μL. The reaction solution was incubated at 28 °C for 2 h, then quenched with absolute methanol. After centrifugation at 15,000 rpm for 10 min, the products were then subjected to LC-MS analysis as mentioned above.

Chemical extraction of native producer *Pseudoalteromonas luteoviolacea* H33 of darobactin A and other analogues. The wild-type strain *Pseudoalteromonas luteoviolacea* H33 was cultivated in M2 medium for 3 days at 30 °C and 180 ppm, as previously described.[2] Composition of M2 medium: KBr (0.1 g/L), $MgCl_2{\cdot}6H_2O$ (10.61 g/L), $CaCl_2{\cdot}2H_2O$ (1.47 g/L), KCl (0.66 g/L), $SrCl_2{\cdot}6H_2O$ (0.04 g/L), Na_2SO_4 (3.92 g/L), $NaHCO_3$ (0.19 g/L), H_3BO_3 (0.03 g/L), MOPS (40 mM), glucose (3.0 g/L), and casein (5.0 g/L). Subsequently, the cells were removed by centrifugation, and the supernatant was concentrated using a 0.5 g C18 SPE column and consecutive evaporation in a GeneVac centrifugal concentrator (SPScientific, Ipswitch, UK). The concentrated crude extract was resuspended in 200 mL H_2O + 0.1 % formic acid and analyzed by UPLC-HR-ESI-MS (Agilent Infinity 1290 UPLC system coupled with a DAD detector and a Bruker Daltonics micrOTOFQ II mass spectrometer equipped with electrospray ionization source).

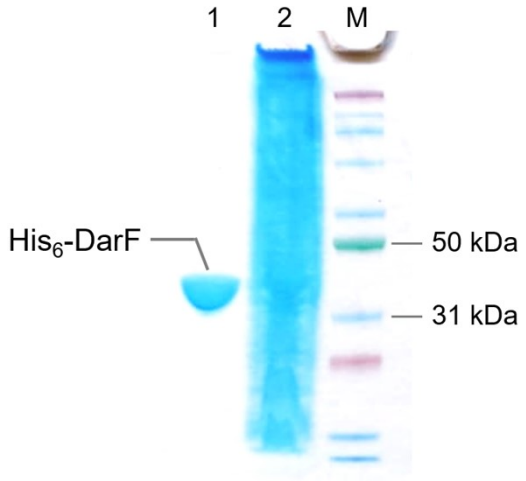

Figure S1. SDS-PAGE of His_6-DarF. M: molecular weight marker. 1: *in vivo* expression of His_6-DarF in *E. coli* NiCo21 (DE3) and Ni-affinity purification to obtain purified His_6-DarF. 2: *in vivo* expression of His_6-DarF in *E. coli* NiCo21 (DE3) and without Ni-affinity purification to obtain unpurified supernatant. Theoretical molecular weight of recombinant His_6-DarF is 43.0 kDa.

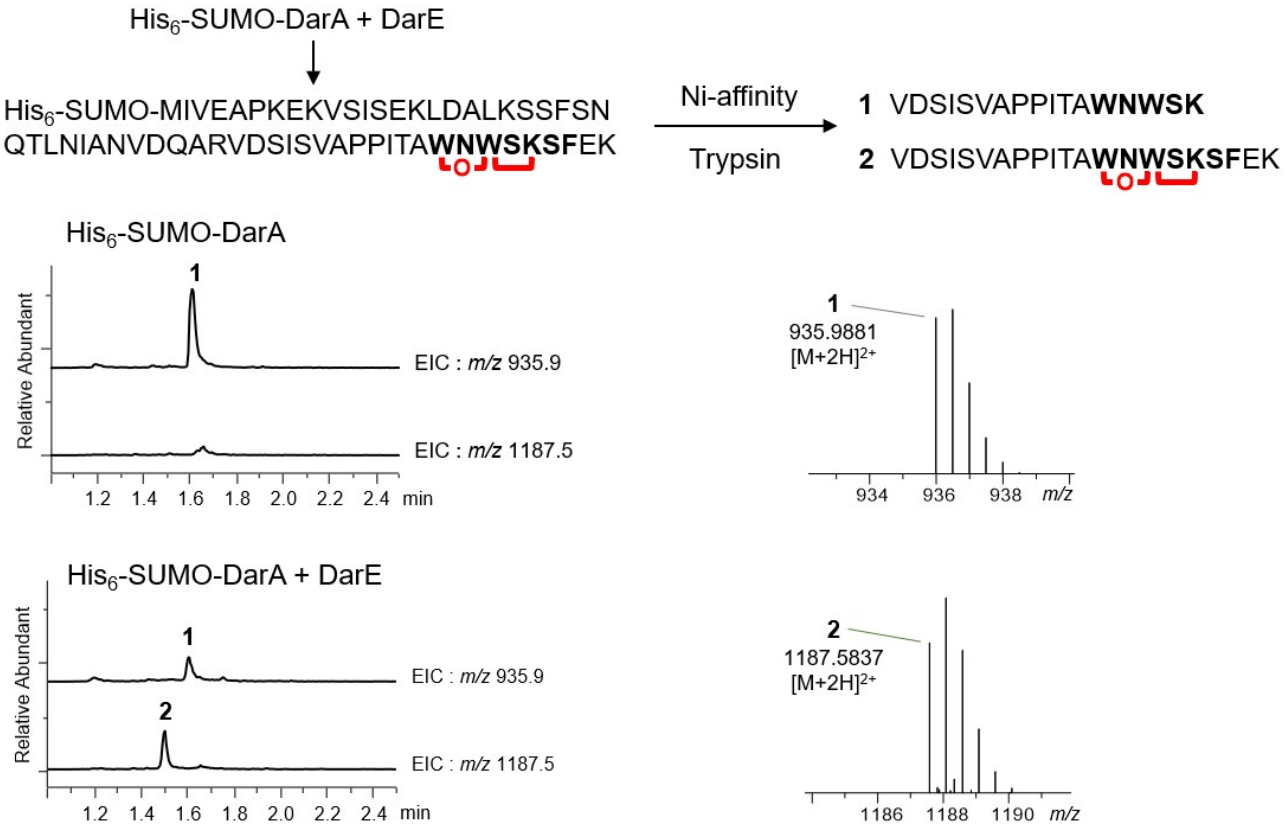

Figure S2. *In vivo* coexpression of His_6-SUMO-DarA + DarE followed by Ni-affinity purification and trypsin digestion yielded fragments **1** and **2**. The EIC chromatogram and MS spectrum of fragments **1** and **2**. Core peptides are shown as bold letters. Cross-link formation on the peptide sequences is shown as red connectors.

Ion	Fragment	Calc.	Obs.	error (ppm)
b2	VD	215.1032	215.1032	0.0930
b3	VDS	302.1352	302.1324	-9.3005
b4	VDSI	415.2193	415.2187	-1.3728
b5	VDSIS	502.2513	502.2486	-5.3758
b6	VDSISV	601.3197	601.3179	-3.0267
b7	VDSISVA	672.3568	672.3558	-1.5319
b8	VDSISVAP	769.4096	769.411	1.8326
b10	VDSISVAPPI	979.5464	979.542	-4.5123
y1	**K**	147.11335	147.1132	-1.0196
y2	**SK**	234.14538	234.1445	-3.7583
y3	**WSK**	420.22469	420.2233	-3.3078
y4	**NWSK**	534.26762	534.2685	1.6471
y5	**WNWSK**	720.34693	720.3464	-0.7358
y6	A**WNWSK**	791.38405	791.3864	2.9695
y7	TA**WNWSK**	892.43173	892.4323	0.6387
y8	ITA**WNWSK**	1005.51579	1005.5212	5.3803
y9	PITA**WNWSK**	1102.56855	1102.564	-4.1267
y10	PPITA**WNWSK**	1199.62132	1199.6208	-0.4335
y11	APPITA**WNWSK**	1270.65843	1270.6565	-1.5189
y12	VAPPITA**WNWSK**	1369.72685	1369.7305	2.6648
y13	SVAPPITA**WNWSK**	1456.75887	1456.7517	-4.9219

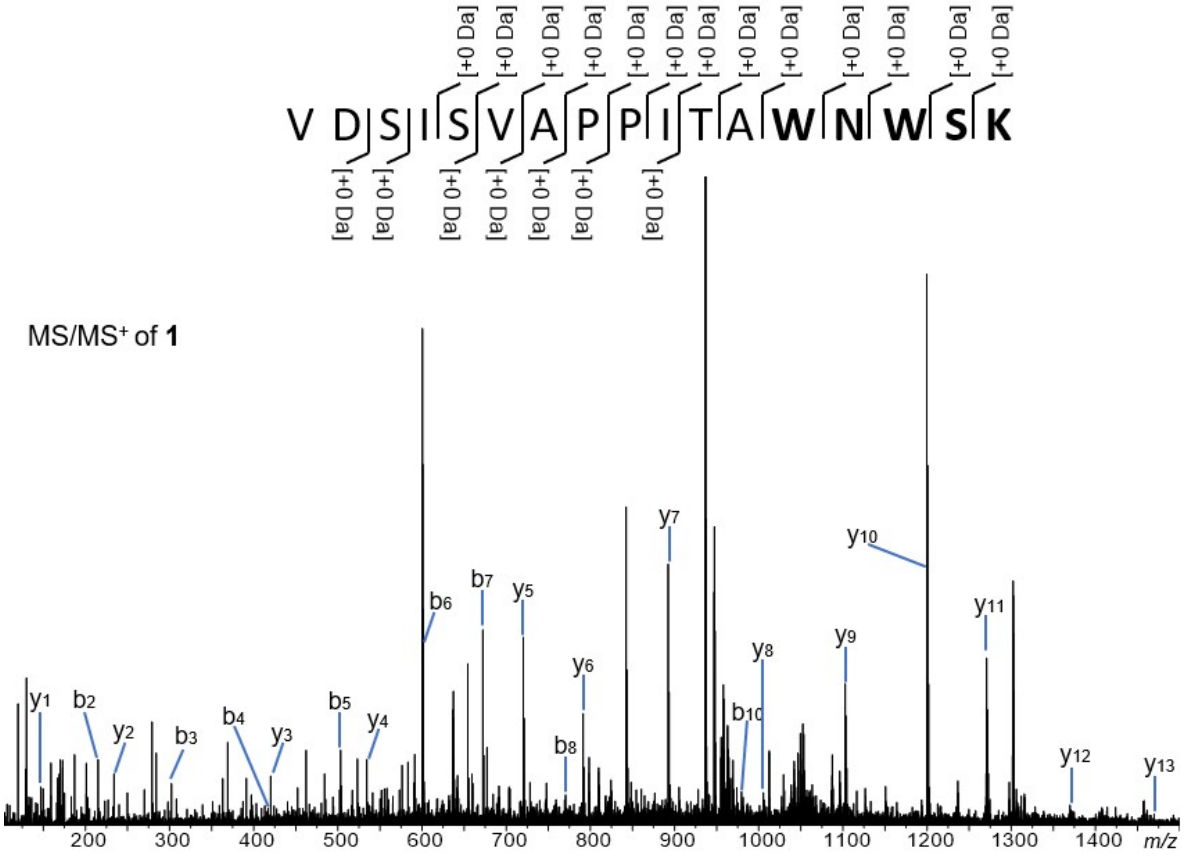

Figure S3. The MS/MS spectrum of fragment **1**.

Ion	Fragment	Calc.	Obs.	error (ppm)
b2	VD	215.10318	215.1021	-5.0208
b3	VDS	302.13521	302.134	-4.0048
b5	VDSIS	502.2513	502.2457	-11.1498
b6	VDSISV	601.31972	601.3139	-9.6787
b7	VDSISVA	672.35683	672.3551	-2.5730
b8	VDSISVAP	769.40959	769.4064	-4.1460
b10	VDSISVAPPI	979.54642	979.5195	-27.4821
b12	VDSISVAPPITA	1151.63121	1151.6218	-8.1710
y1	K	147.11335	147.1128	-3.7386
y2	EK	276.15595	276.1356	-73.6902
y3	FEK	423.22436	423.2187	-13.3735
y4	SFEK	510.25639	510.2535	-5.6638
y9	**WNWSK**SFEK [+12 Da]	1223.54855	1223.5455	-2.4927
y10	A**WNWSK**SFEK [+12 Da]	1294.58566	1294.5792	-4.9900
y11	TA**WNWSK**SFEK [+12 Da]	1395.63334	1395.6321	-0.8885
y12	ITA**WNWSK**SFEK [+12 Da]	1508.7174	1508.7268	6.2305
y13	PITA**WNWSK**SFEK [+12 Da]	1605.77017	1605.7687	-0.9154
y14	PPITA**WNWSK**SFEK [+12 Da]	1702.82293	1702.8099	-7.6520

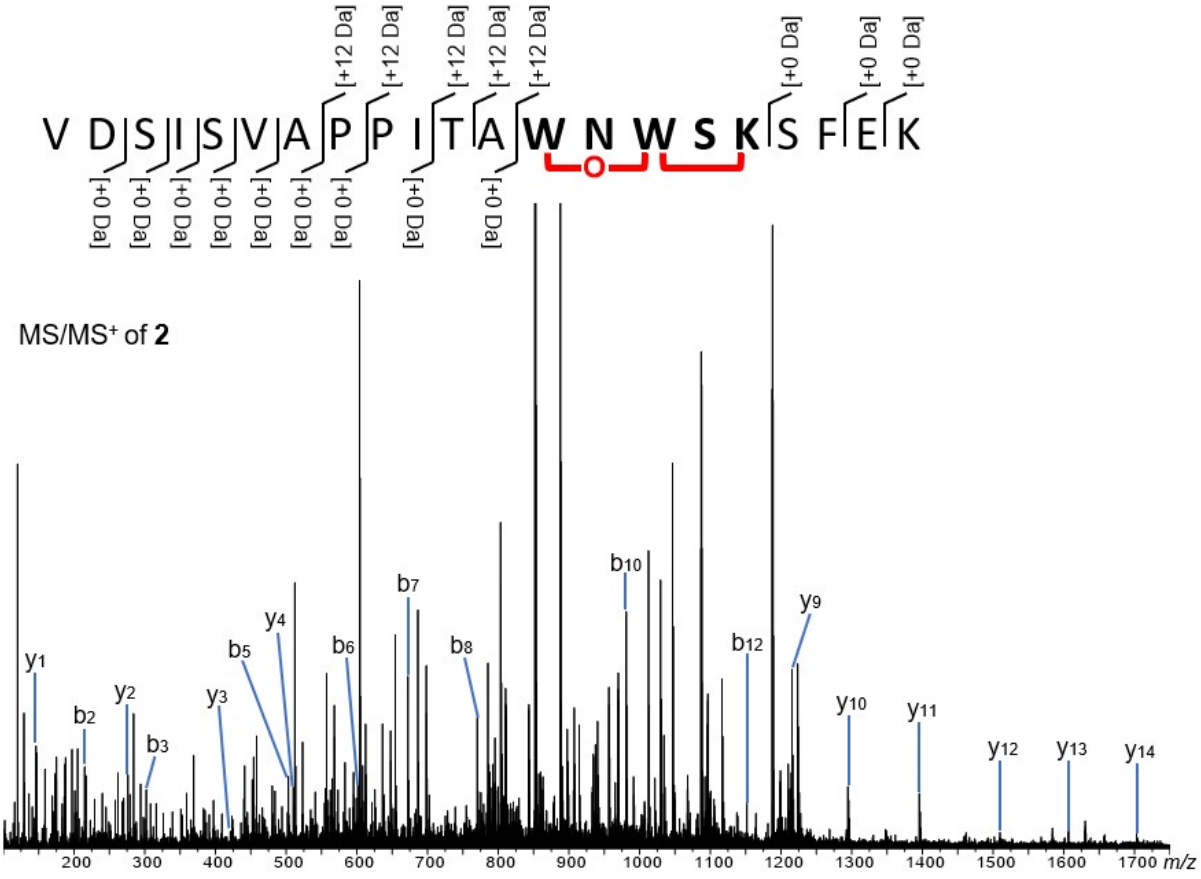

Figure S4. The MS/MS spectrum of fragment **2**.

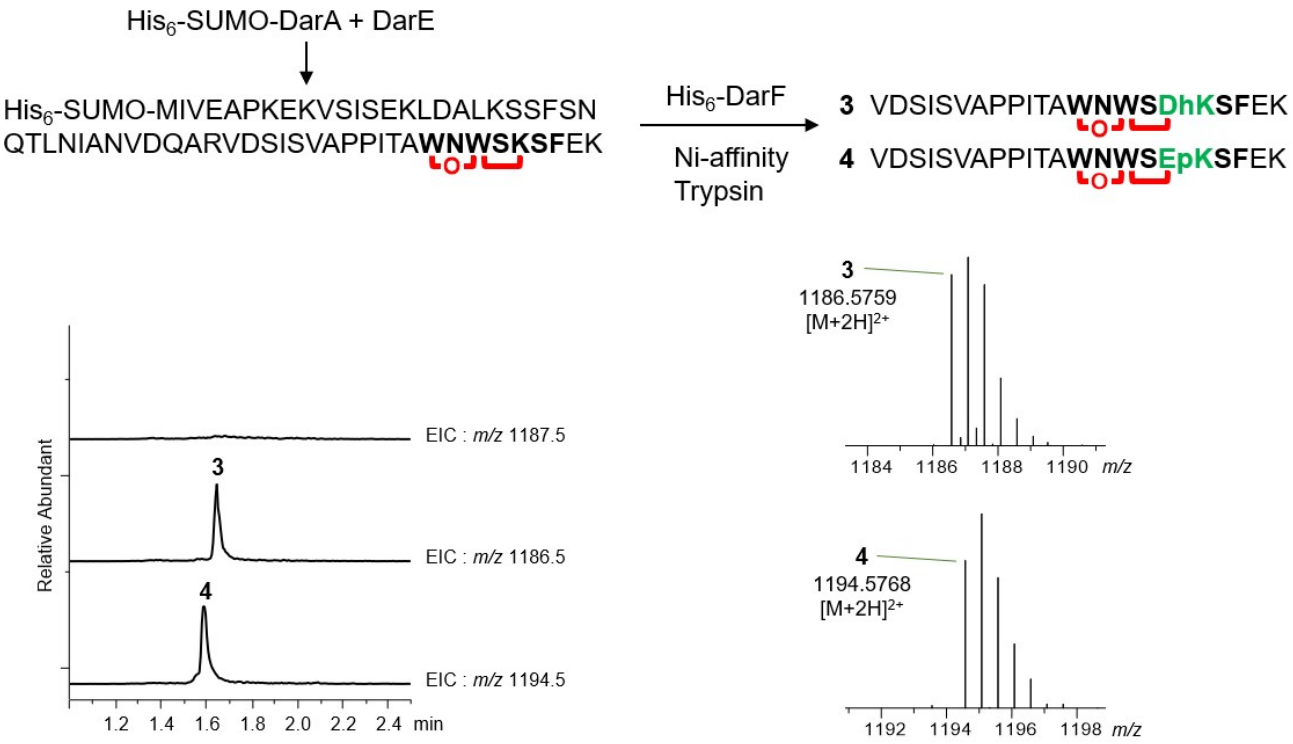

Figure S5. *In vitro* assay of His_6-DarF + modified full-length His_6-SUMO-DarA. The EIC chromatogram and MS spectra of fragments **3** and **4**. Core peptides are shown as bold letters. Cross-link and DarF transformation on the peptide sequences is shown as red connecters and green colored letters, respectively.

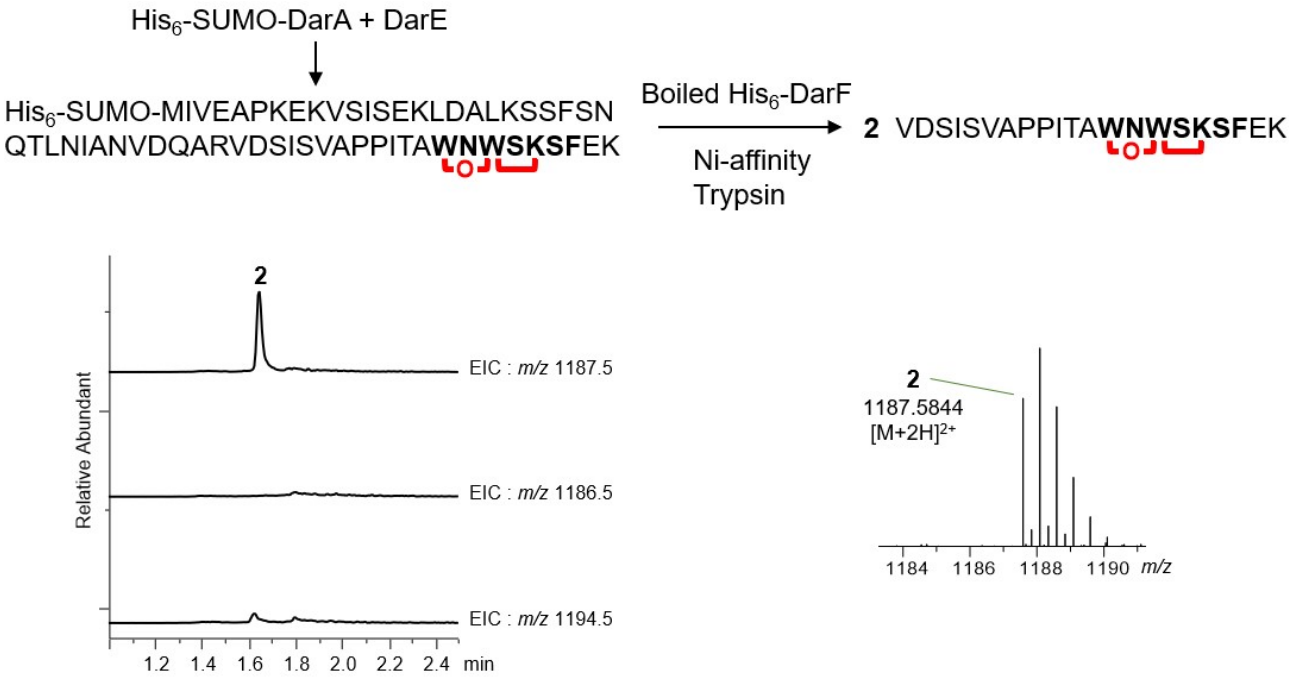

Figure S6. *In vitro* assay of boiled His_6-DarF + modified full-length His_6-SUMO-DarA. The EIC chromatogram and MS spectrum of fragment **2**. Core peptides are shown as bold letters. Cross-link on the peptide sequences is shown as red connecters.

Ion	Fragment	Calc.	Obs.	error (ppm)
b2	VD	215.10318	215.1034	1.0228
b3	VDS	302.13521	302.1339	-4.3358
b4	VDSI	415.21927	415.2143	-11.9696
b5	VDSIS	502.2513	502.25	-2.5883
b6	VDSISV	601.31972	601.3207	1.6297
b7	VDSISVA	672.35683	672.3567	-0.1933
b8	VDSISVAP	769.40959	769.4053	-5.5757
b10	VDSISVAPPI	979.54642	979.4728	-75.1572
b11	VDSISVAPPIT	1080.5941	1080.5873	-6.2928
b12	VDSISVAPPITA	1151.63121	1151.6309	-0.2692
y1	K	147.11335	147.1133	-0.3399
y2	EK	276.15595	276.1526	-12.1308
y3	FEK	423.22436	423.2207	-8.6479
y4	SFEK	510.25639	510.2531	-6.4477
y9	**WNWS**DhKSFEK [+10 Da]	1221.5329	1221.5342	1.0642
y10	A**WNWS**DhKSFEK [+10 Da]	1292.57001	1292.5802	7.8835
y11	TA**WNWS**DhKSFEK [+10 Da]	1393.61769	1393.6113	-4.5852
y13	PITA**WNWS**DhKSFEK [+10 Da]	1603.75452	1603.8048	31.3514
y14	PPITA**WNWS**DhKSFEK [+10 Da]	1700.80728	1700.799	-4.8683

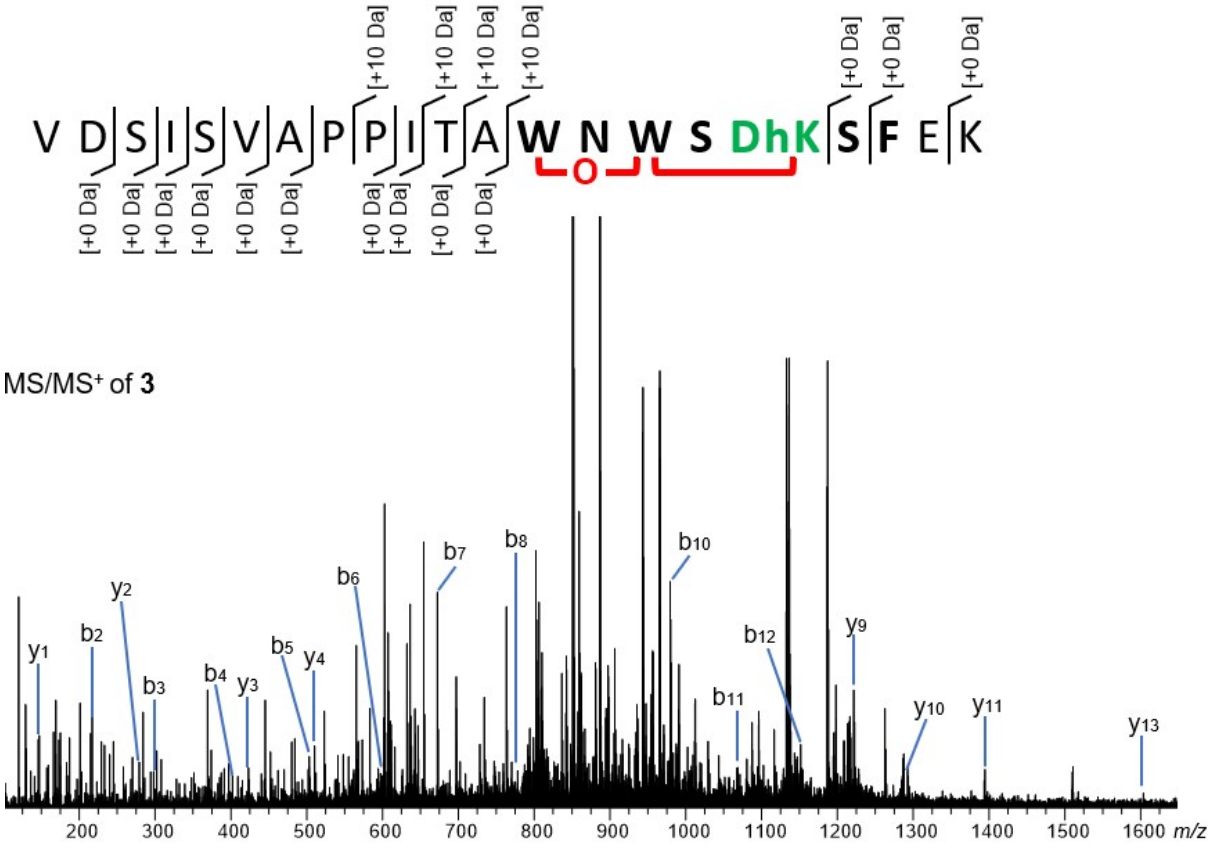

Figure S7. The MS/MS spectrum of fragment **3**.

Ion	Fragment	Calc.	Obs.	error (ppm)
b2	VD	215.10318	215.1021	-5.0208
b3	VDS	302.13521	302.1343	-3.0119
b4	VDSI	415.21927	415.2205	2.9623
b6	VDSISV	601.31972	601.313	-11.1754
b7	VDSISVA	672.35683	672.3544	-3.6142
b12	VDSISVAPPITA	1151.63121	1151.629	-1.9190
y1	K	147.11335	147.1123	-7.1374
y3	FEK	423.22436	423.2231	-2.9771
y4	SFEK	510.25639	510.2597	6.4869
y9	**WNWS**EpKSFEK [+26 Da]	1237.52781	1237.5317	3.1434
y10	A**WNWS**EpKSFEK [+26 Da]	1308.56493	1308.5665	1.1998
y11	TA**WNWS**EpKSFEK [+26 Da]	1409.6126	1409.6077	-3.4761
y13	PITA**WNWS**EpKSFEK [+26 Da]	1619.74943	1619.7322	-10.6374
y14	PPITA**WNWS**EpKSFEK [+26 Da]	1716.8022	1716.7845	-10.3099

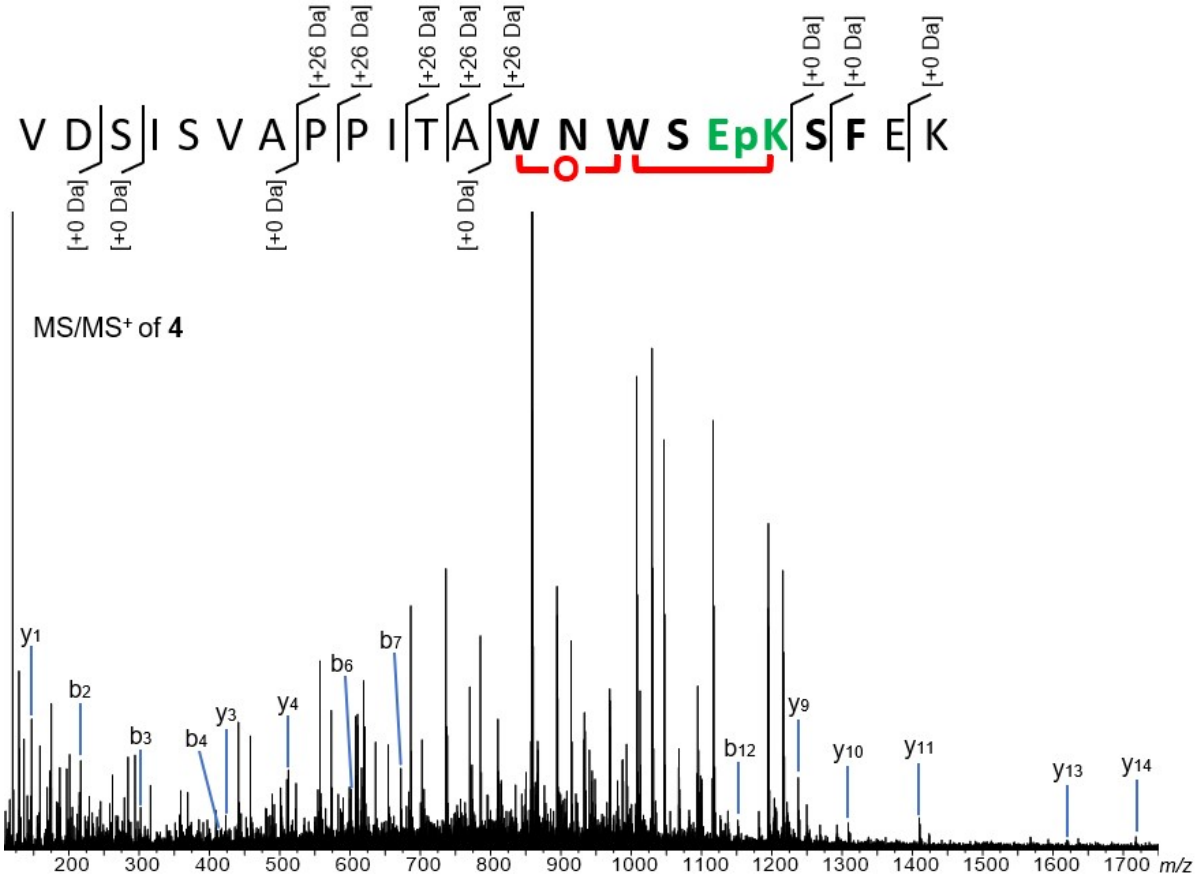

Figure S8. The MS/MS spectrum of fragment **4**.

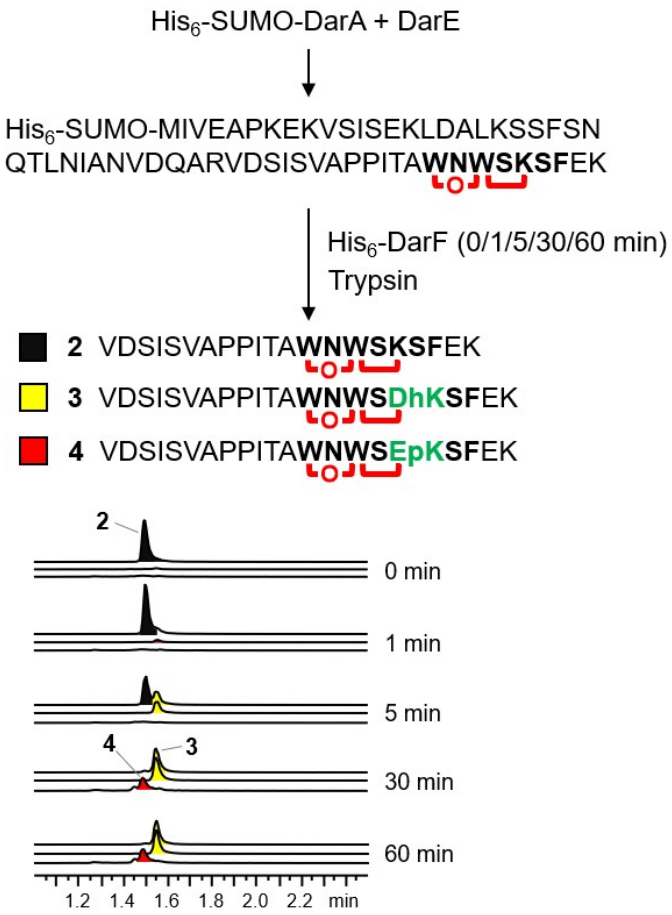

Figure S9. Time-course *in vitro* assay of His_6-DarF. Core peptides are shown as bold letters. Cross-link and DarF transformation on the peptide sequences is shown as red connecters and green colored letters, respectively. EIC of peptide fragments **2** (*m/z* 1187.5), **3** (*m/z* 1186.5) and **4** (*m/z* 1194.5) are indicated in first, second and third lines in the chromatogram. EIC of peaks **2**, **3** and **4** are colored as black, yellow and red.

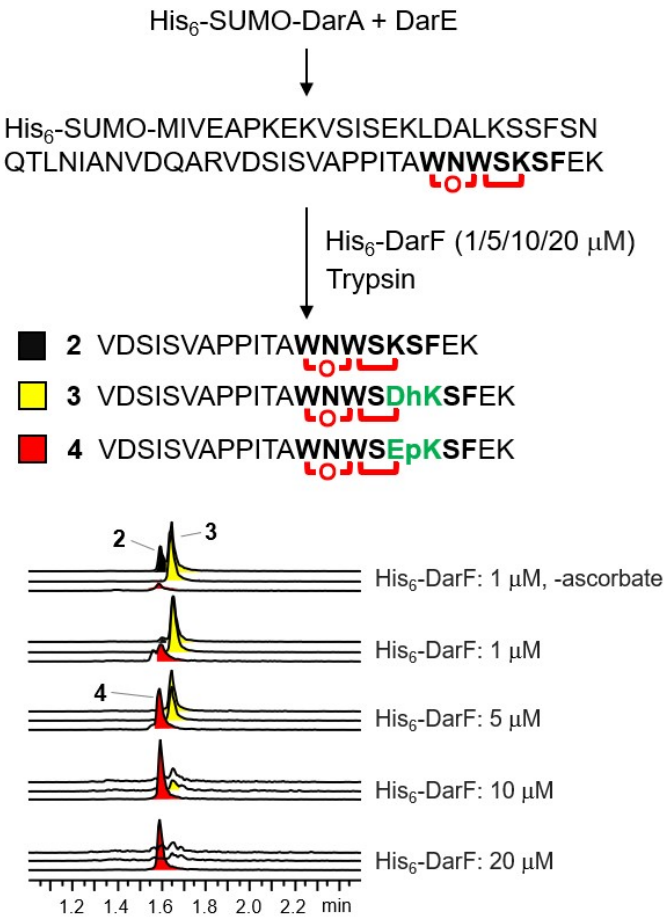

Figure S10. Enzyme concentration-dependent *in vitro* assay of His_6-DarF. Experiment without addition of ascorbate resulted an incomplete conversion of **2** to **3**/**4**. Core peptides are shown as bold letters. Cross-link and DarF transformation on the peptide sequences is shown as red connecters and green colored letters, respectively. EIC of peptide fragments **2** (*m/z* 1187.5), **3** (*m/z* 1186.5) and **4** (*m/z* 1194.5) are indicated in first, second and third lines in the chromatogram. EIC of peaks **2**, **3** and **4** are colored as black, yellow and red.

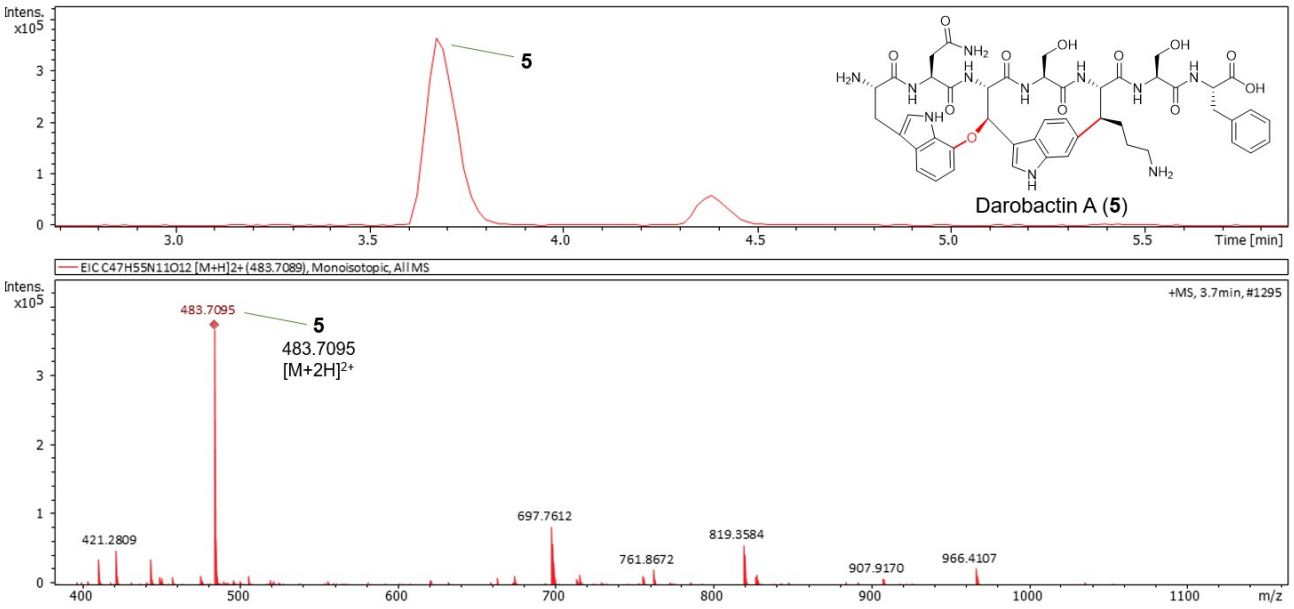

Figure S11. The EIC chromatogram and MS spectrum of darobactin A (**5**) from chemical extraction of *Pseudoalteromonas luteoviolacea* H33. HR-MS *m/z* $[M+2H]^2$ calculated for $C_{47}H_{55}N_{11}O_{12}$ 483.7089; observed 483.7085; error in ppm -0.83.

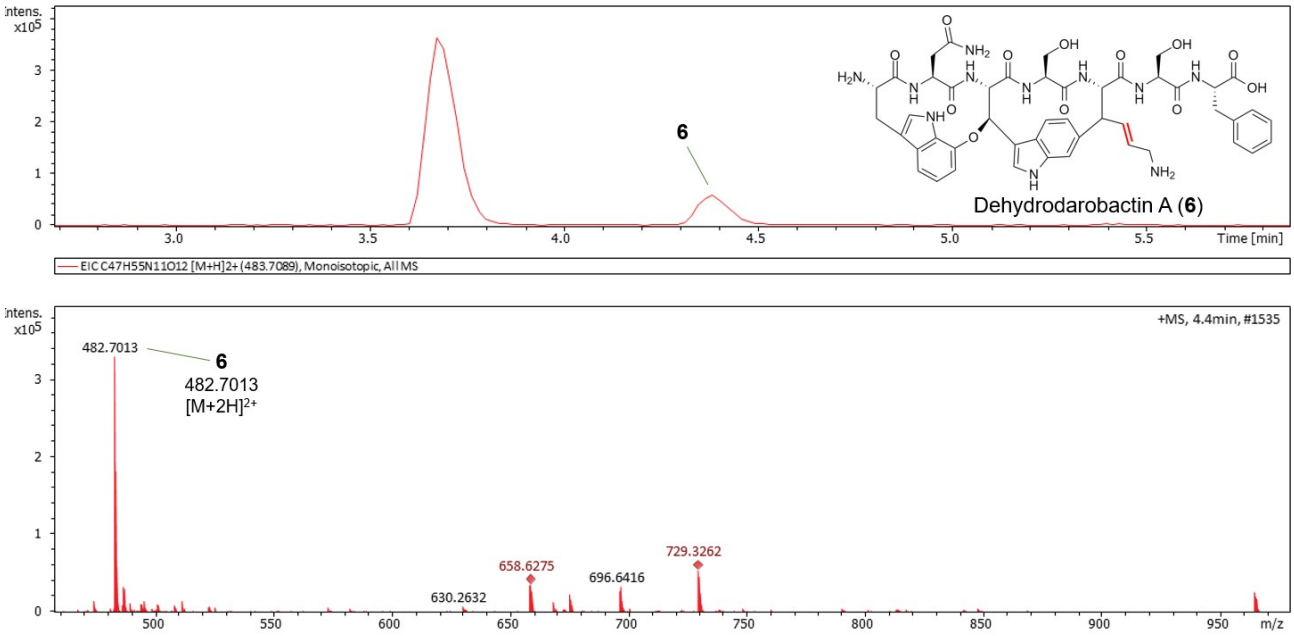

Figure S12. The EIC chromatogram and MS spectrum of dehydrodarobactin A (**6**) from chemical extraction of *Pseudoalteromonas luteoviolacea* H33. HR-MS *m/z* $[M+2H]^2$ calculated for $C_{47}H_{53}N_{11}O_{12}$ 483.7010; observed 482.7013; error in ppm 0.62.

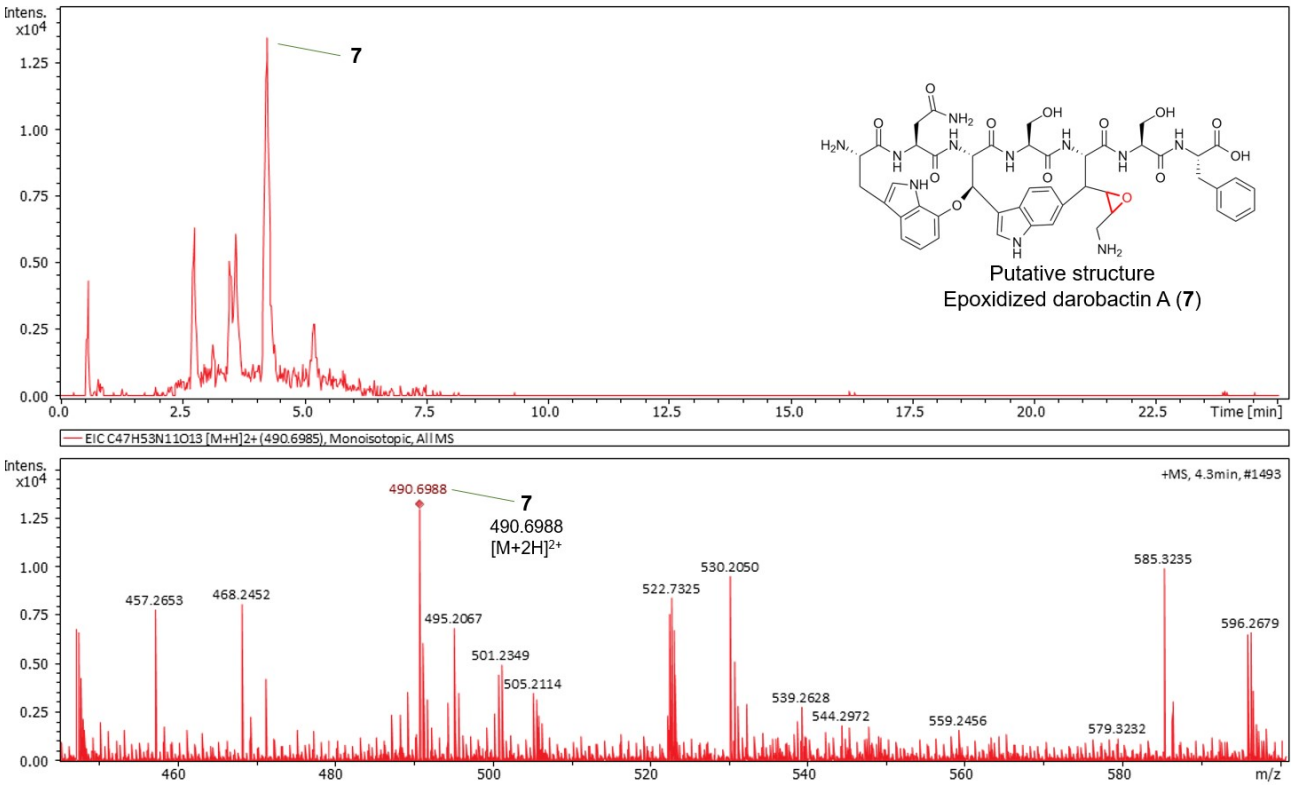

Figure S13. The EIC chromatogram and MS spectrum of epoxidized darobactin A (**7**) from chemical extraction of *Pseudoalteromonas luteoviolacea* H33. HR-MS *m/z* $[M+2H]^2$ calculated for $C_{47}H_{53}N_{11}O_{13}$ 490.6985; observed 490.6988; error in ppm 0.61.

No:	Chain	Z	rmsd	lali	nres	%id	PDB	Description
1:	8s5f-A	23.3	3.5	292	342	13		MOLECULE: CHLH FROM CHLOROGLOEOPSIS SP.;
2:	5xbn-A	7.3	3.3	111	128	12		MOLECULE: WSS1P;
3:	4l7a-A	6.3	4.9	151	261	10		MOLECULE: UNCHARACTERIZED PROTEIN;
4:	5n0c-A	6.2	3.7	150	1293	13		MOLECULE: TETANUS TOXIN;
5:	9b6m-A	6.1	4.4	147	390	11		MOLECULE: PG1 LIGHT CHAIN;
6:	3e11-A	5.8	2.4	82	114	15		MOLECULE: PREDICTED ZINCIN-LIKE METALLOPROTEASE;
7:	8qft-A	5.8	3.8	153	1174	8		MOLECULE: NON-TOXIC NON-HEMAGGLUTININ PROTEIN X;
8:	1z1w-A	5.7	5.5	132	780	4		MOLECULE: TRICORN PROTEASE INTERACTING FACTOR F3;
9:	6mzc-B	5.5	4.2	159	968	6		MOLECULE: TRANSCRIPTION INITIATION FACTOR TFIID SUBUNIT 2;
10:	7v9o-A	5.4	4.2	155	860	12		MOLECULE: ALANINE AMINOPEPTIDASE;
11:	8d2j-B	5.3	3.9	115	483	8		MOLECULE: IPD113_COW;
12:	4fgm-A	5.3	4.1	156	587	10		MOLECULE: AMINOPEPTIDASE N FAMILY PROTEIN;
13:	7y7o-A	5.3	3.3	107	147	9		MOLECULE: ENDORIBONUCLEASE YBEY;
14:	7pfs-A	5.2	4.2	156	916	10		MOLECULE: ENDOPLASMIC RETICULUM AMINOPEPTIDASE 2;
15:	2h1n-A	5.2	4.5	148	566	10		MOLECULE: OLIGOENDOPEPTIDASE F;
16:	6ggo-A	5.2	4.0	131	199	9		MOLECULE: BACTERIOPHAGE VIRULENCE DETERMINANT;
17:	1vct-A	5.2	2.6	71	193	6		MOLECULE: HYPOTHETICAL PROTEIN PH0236;
18:	7c79-L	5.2	3.1	85	131	6		MOLECULE: RIBONUCLEASE MRP RNA SUBUNIT NME1;
19:	1sum-B	5.1	3.0	71	224	8		MOLECULE: PHOSPHATE TRANSPORT SYSTEM PROTEIN PHOU HOMOLOG 2
20:	8c8g-A	5.0	4.6	158	1335	16		MOLECULE: PUTATIVE BOTULINUM-LIKE TOXIN WO;

Figure S14. Top 20 DALI[12] hits of DarF structure predicted by AlphaFold3.[13] The output results indicate that the HExxH enzyme ChlH (PDB: 8S5F)[8] is structurally most similar to DarF, as shown in red bracket.

Figure S15. A sequence alignment generated using Multalin version 5.4.1.[14] Conserved HExxH and PWRxxxRP motifs are shown in green brackets. Aligned αKG-dependent HExxH enzymes, $MscH_{429-768}$ (WP_013477425.1),[8] $SjiH_{460-819}$ (WP_042453644.1),[8] $ChlH_{376-722}$ (WP_016869186.1),[8] and DarF (WP_063364329.1).[2] The C-terminal HExxH domains in MscBH, SjiBH and ChlBH are referred to as MscH, SjiH and ChlH, respectively.

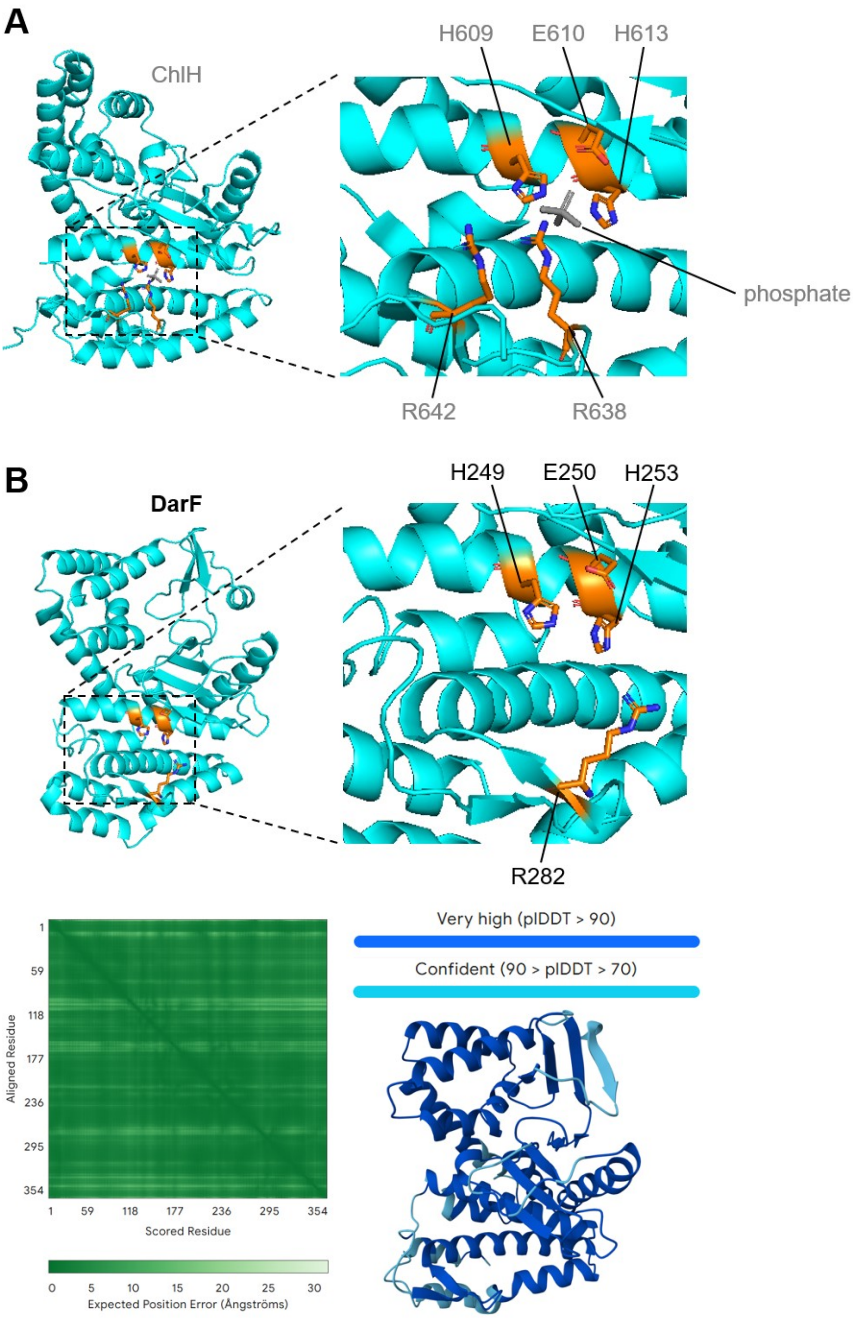

Figure S16. Overview of HExxH and PWRxxxRP motifs in αKG-dependent HExxH enzymes. (A) The crystal structure of N-terminal His_6 tag ChlH (PDB: 8S5F).[8] (B) The predicted structure of DarF by AlphaFold3,[13] and confidence measure of PAE for modeling.

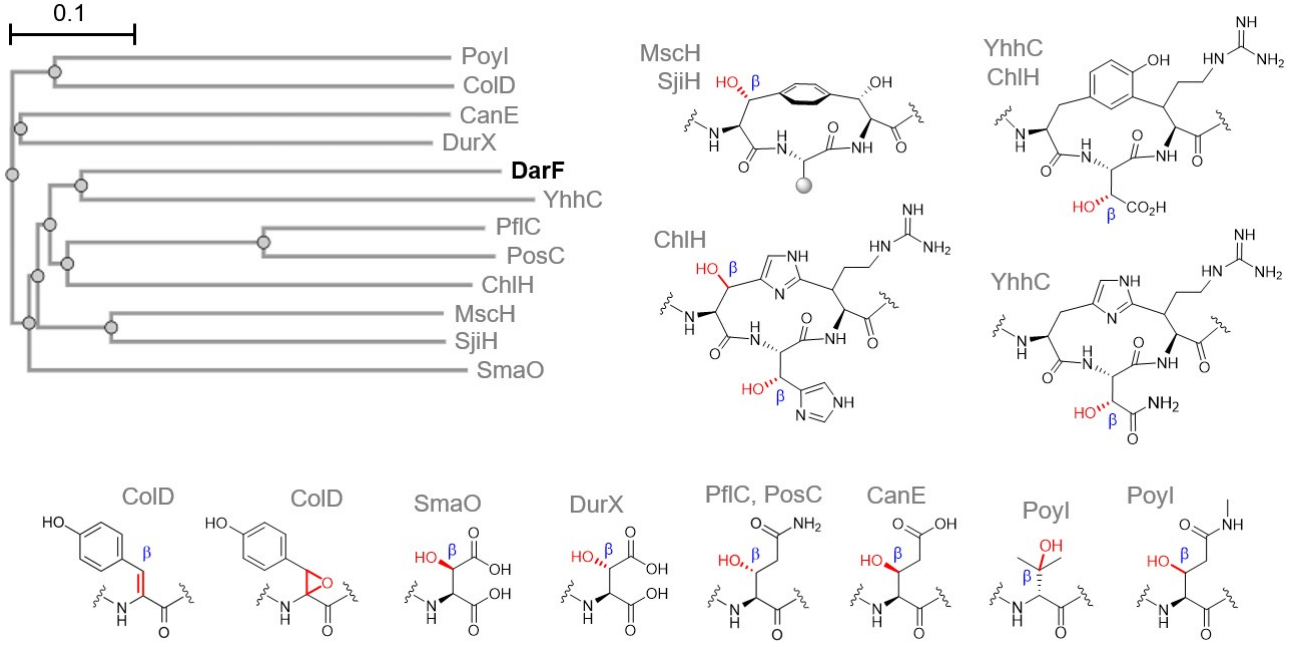

Figure S17. The reactions of RiPP αKG-dependent enzymes and their phylogenetic tree generated from Clustal Omega multisequence alignment of PoyI (AFS60645.1),[3] DurX (WP_071962208.1),[4] CanE (KUN61407.1),[5] YhhC (WP_003708570.1),[6] SmaO (WP_141401631.1),[7] $MscH_{429\text{-}768}$ (WP_013477425.1),[8] $SjiH_{460\text{-}819}$ (WP_042453644.1),[8] $ChlH_{376\text{-}722}$ (WP_016869186.1),[8] PflC (WP_192559974.1),[9] PosC (WP_060837885.1),[9] ColD (WP_033308454.1),[10] and DarF (WP_063364329.1).[2] Known enzymes and DarF (this study) are shown as grey and bold black colored letters, respectively. The enzymatic reactions in the structures are shown as red colored bonds.

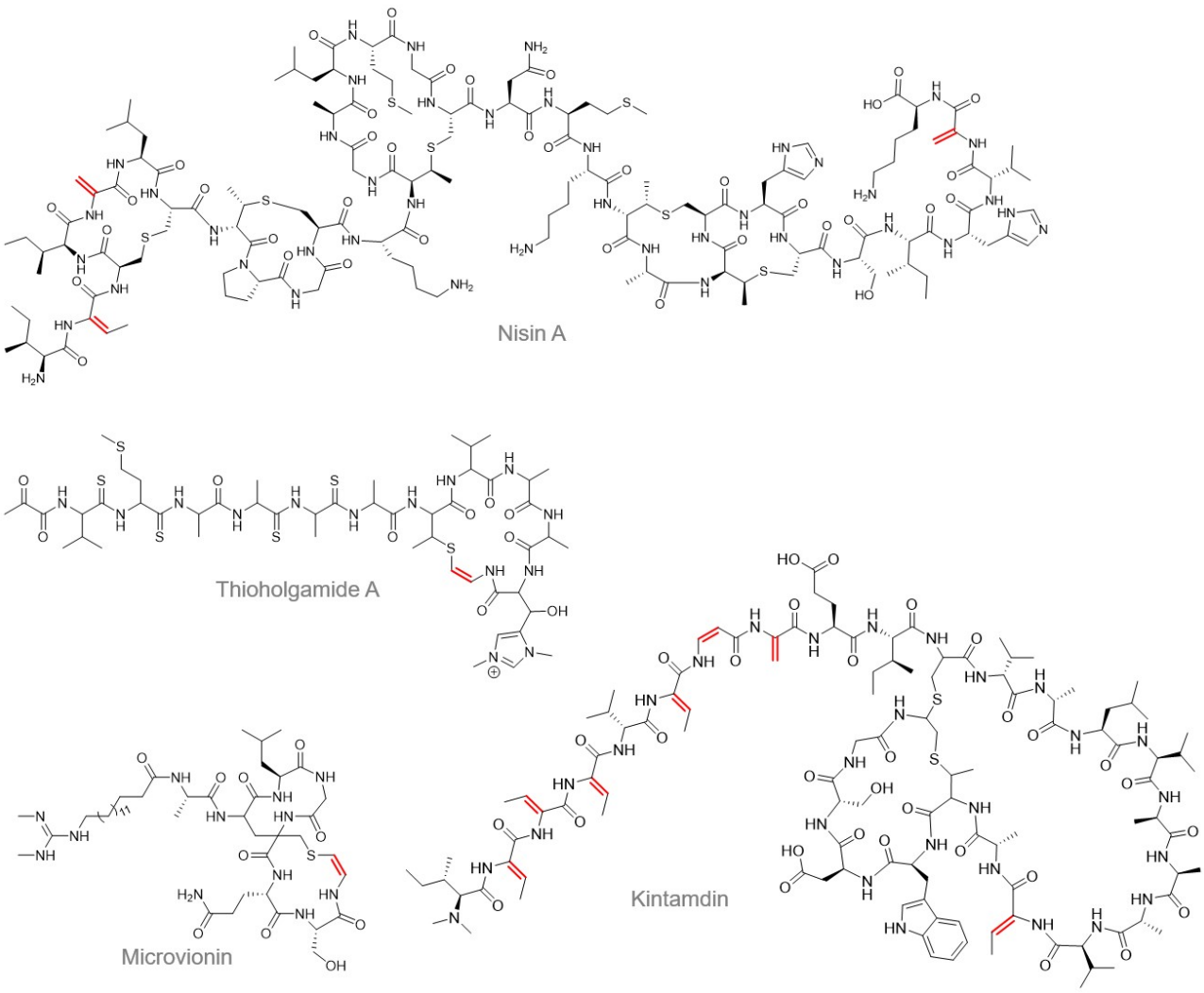

Figure S18. Representative examples of lanthipeptides containing dehydroamino acids such as nisin A,[15] thioholgamide A,[16] microvionin[17] and kintamdin.[18] Desaturated formation on the structure is shown as red bonds.

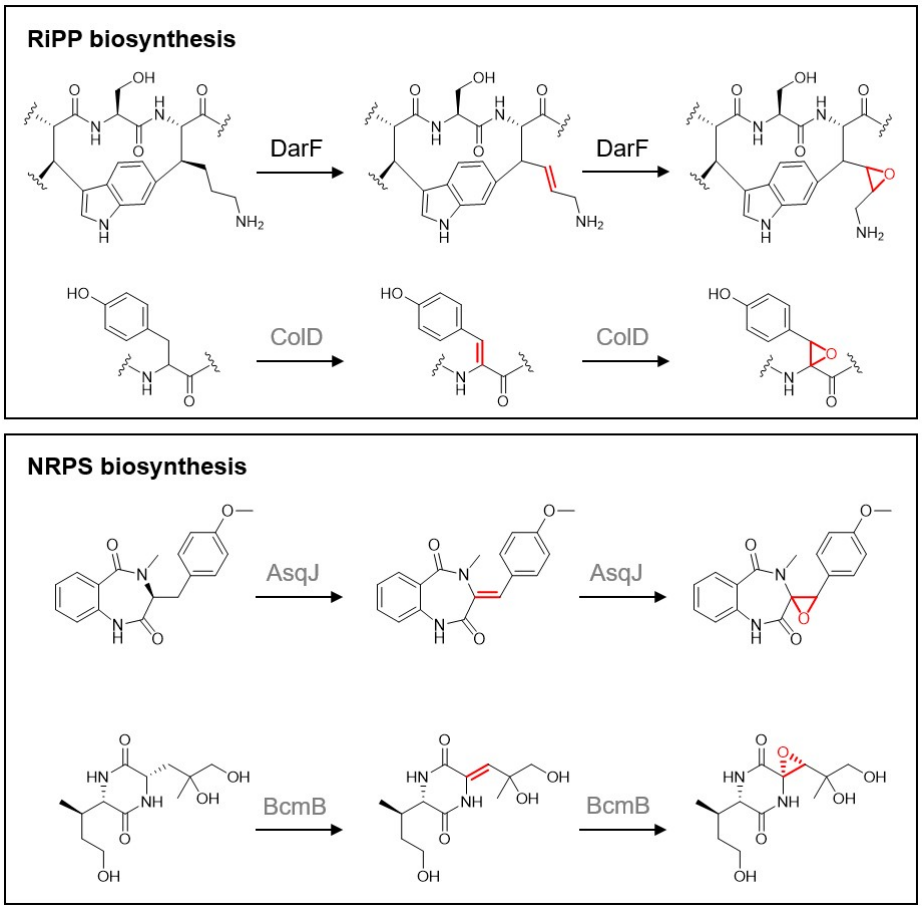

Figure S19. Overview of αKG-dependent enzymes catalyzed dehydrogenation and epoxidation in RiPP and non-ribosomal peptide synthetase (NRPS) biosynthesis. DarF from the darobactin biosynthesis in bacterial RiPP. ColD from the collinodin biosynthesis in bacterial RiPP.[10] AsqJ from the viridicatin biosynthesis in fungal NRPS.[19] BcmB from the bicyclomycin biosynthesis in bacterial NRPS.[20] Desaturated and epoxide formation on the structure is shown as red bonds. Known enzymes and DarF (this study) are shown as grey and bold black colored letters, respectively.

Table S1. Gene sequences used in this study.

Gene	Vector (Restriction Sites)	Insert Sequence[b]
DarA WP_155731785.1	pET28a(+) NcoI(-G)/XhoI	ggcagcagccatcatcaccaccatcacgggtccctgcaggactcagaagtcaa tcaagaagctaagccagaggtcaagccagaagtcaagcctgagactcacatc aatttaaaggtgtccgatggatcttcagagatcttcttcaagatcaaaaagaccact cctttaagaaggctgatggaagcgttcgctaaaagacagggtaaggaaatgga ctccttaacgttcttgtacgacggtattgaaattcaagctgatcagacccctgaaga tttggacatggaggataacgatattattgaggctcaccgcgaacagattggaggt ATTGTTGAAGCGCCAAAAGAAAAGGTCTCCATCTCCGA AAAGTTGGACGCACTGAAGTCGTCGTTCTCTAACCAAA CCTTAAATATTGCAAATGTGGACCAAGCGCGCGTTGAC TCCATATCCGTGGCTCCACCCATTACAGCATGGAACTG GTCCAAATCTTTCGAGAAATAAGAATTCCGAGTTCTGGT TCGTCCGAGCGGAGCCGCAGATTGAGACCAACTGGTG ACAAGACTTCTCCTGAATACATTCTTCCTGCCTAGTAGC GGGTGATAATGGTTACTTCCCGCCGGAGTAGAA
DarE WP_063364333.1	pCDFDuet-1 NdeI_XhoI	CTGGGCGATATTAGCGTCAAAGTGATTGAGGAGCCGG TTAATCCTGTTAACCAACTCGAATTGACTGACTACCAGT ACTCTCGTCTGGCTTCGCAACTTATAGGCGAGATCCCA GACAGTGACATGTTGGACGAAGAGGAGCTCGCCCTCT TTCGACGGGAGAAGGACGCCTACTTCGAGGCCAAACC CCTGAACGCGAGCAAGGTCGTGGTTGTGTTGAAAGCTA CGAGACTGTGCAACTTACGCTGTACATACTGCCACTCT TGGGCCGAGGGCCCAAACCAAACTGTAAAATTCGAGAA CCTGATTTCCATTGTCAAGCGTATTCTGGCCATCCCGA ATGTAAGTCGGGTTGAATTCGTTTGGCACGGCGGTGAA GTGACATTATTACGCCCTGCCTTCTTCAAGAAACTTATC TGGCTGCAAGAGCAATTCAAGCGTAAGGATCACTTCAT CACCAATACGATGCAATCCAATGCGGTGAACATCTCCA AGGAGTGGCTTACATTTCTGCAGGGTATTGGTATGGCC GTCGGCATTTCGTTCGATGGCGTTCCAGAAATCAACGA TACACGTCGCCTTGACGTTAGAGGGCGACCGACATCCT TAAAGGTAGCAGAGGGCATCAAACGTCTGCAAGAATAC GGTATACCCTATGGCGCTTTAATCGTCGTAGATCGGGA CGTCTACAATGTATCACCGGAGAGACTGTTGAGTTATC TCGCTAGCATCGAACTCAATGACATCGAGTTCTTAAACA TCGTACCAGATAACCGCGCGCAACCCGGCGATGACAT CGGAGATGCCTACATTAGTTACAAAGAATATATAGAGTT CCTCAGCCGTGTTTATACTGTGTGGCATGCCCAGTACC GCGGGATAATACAAATACGCATGTTTGAGAACTTCATG GACGTTCTGGCGGATCGGAGTAAGCAATTGTCCGCTTG CTATTGGGCTGGCAATTGTAGTCAAGAAATTATAACCAT TGAGCCGAACGGCGATGTGAGCCCATGTGACAAGTAT GTAGGTGATATAGGATCAATCTATGGATCTTTGCTTGAT TCGGATCTGGCTACCCTGCTGGCTGACTCGAAGCATAA CCAAACATCTGTCTTAGAGGAAGTCGAGAGTCACTCTC GCATGCACGAGTGTAAGTGGTTCTCTATTTGCAACGGT GGATGTCCTCACGACCGGGTGATCAACGCTCGCCACG TTGAGGATTATGACGACAAGTGTTGCGGTACTGGAAAG CTTTTGAAAGTCATTGAAGAGAGTATTTGA
DarF	pET28a(+)	AACACGTTAACGAACGAGCTCCCGAAGTGTTTAGAGTT

WP_063364329.1	NdeI_XhoI	CAACTCAGACAACTTTGCGGATATCTTTTCTCAATGTAA GATTGACCTGCTCGTGGACATCTTCAAACGCGAGATCC TGTCACACAAGGAGTTGTCAGAGTTGTTCGATAAGTTG TCAAACACATTCTCATCAGAAGAGCTGTATCATTTCTTT AAGTTGCCGAAGTTGTGGAAGGTTATATTTACCAGCCG CGGAAAAGATAATTATATCGATAACATTAAGGCTCTTTT CTTGAACGAGCTGAAGGTAGCGGAACTCGATAACCAC GCCATTTCCAACTCCGCGTTGATAGAGCAACCTCAGCT GATATGGAATCTCCGTTCAGACATCGCGTATAACCCAC TGACGCAAAAGGCTTACAAGAACAATTACCAACACAAG GAGACGGGTATTATCATCGACTACTTTTCTGACCTTGCA CGCGGTGAACAGCGGGATATCCCGTGGGGTGACACAG GAATTTCCCAATGCCTGATCGACAACACGGCCCCGAAG GTAACCTCTGCAATTGATTACATACAAAGTGTATCACCG GCATGTTTCAATGTACTTAAAGCGAGTATTTACAGCATC GTGGTCCGCTTCGATACAACGAAGAACATCTTCAACTG CGCATCTACGAACATATGCAATGGTTTAGTGGTATTAAT TAATCCTCACTTAAACGAGGTGTCTGTCGAAACACTTG CCGATGCGATCGTCCATGAGATGACACACAACCTTTTC GATATAGCAGAACTCTACGAACCATGCCTGCCAACGAA GTTCCATCCACAAACAATCAAGTCTCCGTGGACTGGAC GCATGCTGGACCCTAACACTTACATTCAGGCCTGTTAT ACATGGTATGGGCTCCGCAACTTCTGGCAAAAGGCATA CAAGCACTTCAATACTGAGAACGCGCATAAGTACTTGC AGCAGGCGTCTAAGGGCTTCGAGCAGGCAGAGTTCGT AAGAATCGCTAAGAATAGTGATGAAATTATTAATACCAA GTTGATTACAACCTTGGAGAGATTAAAATGA

[a]Codons were optimized for heterologous expression in *E. coli*. [b]His_6-SUMO tag sequence was described in blue colored letters.

Table S2. Amino acid sequence of protein/peptide used in this study.

Protein	sequence
DarE	MLGDISVKVIEEPVNPVNQLELTDYQYSRLASQLIGEIPDSDMLDEEELALFRR EKDAYFEAKPLNASKVVVVLKATRLCNLRCTYCHSWAEGPNQTVKFENLISIVK RILAIPNVSRVEFVWHGGEVTLLRPAFFKKLIWLQEQFKRKDHFITNTMQSNAV NISKEWLTFLQGIGMAVGISFDGVPEINDTRRLDVRGRPTSLKVAEGIKRLQEY GIPYGALIVVDRDVYNVSPERLLSYLASIELNDIEFLNIVPDNRAQPGDDIGDAYI SYKEYIEFLSRVYTVWHAQYRGIIQIRMFENFMDVLADRSKQLSACYWAGNCS QEIITIEPNGDVSPCDKYVGDIGSIYGSLLDSDLATLLADSKHNQTSVLEEVESH SRMHECKWFSICNGGCPHDRVINARHVEDYDDKCCGTGKLLKVIEESI
DarF	MNTLTNELPKCLEFNSDNFADIFSQCKIDLLVDIFKREILSHKELSELFDKLSNTF SSEELYHFFKLPKLWKVIFTSRGKDNYIDNIKALFLNELKVAELDNHAISNSALIE QPQLIWNLRSDIAYNPLTQKAYKNNYQHKETGIIIDYFSDLARGEQRDIPWGDT GISQCLIDNTAPKVTSAIDYIQSVSPACFNVLKASIYSIVVRFDTTKNIFNCASTNI CNGLVVLINPHLNEVSVETLADAIVHEMTHNLFDIAELYEPCLPTKFHPQTIKSP WTGRMLDPNTYIQACYTWYGLRNFWQKAYKHFNTENAHKYLQQASKGFEQA EFVRIAKNSDEIINTKLITTLERLK
DarA	MIVEAPKEKVSISEKLDALKSSFSNQTLNIANVDQARVDSISVAPPITA**WNWSKS F**EK

Table S3. Strains used in this study.

Strains	Description
E. coli DarA	*E. coli* NiCo (DE3) harboring DarA-pET28a(+)
E. coli DarA + DarE	*E. coli* NiCo (DE3) harboring DarA-pET28a(+) and DarE-pCDFDuet-1
E. coli DarF	*E. coli* NiCo (DE3) harboring DarF-pET28a(+)
Pseudoalteromonas luteoviolacea H33 [a]	Wild-type strain. This strain was previously provided by Lone Gram[21] to Nils Böhringer and Till F. Schäberle.

[a]Wild-type strain, native producer of darobactin A, bromodarobactin A, dehydrobromodarobactin A, and dehydrodarobactin A, where their structures have been verified by NMR and HR-MS.[2]

References

1. Altschul, S. F.; Gish, W.; Miller, W.; Myers, E. W.; Lipman, D. J. Basic local alignment search tool. *J. Mol. Biol.* **1990**, *215*, 403–410.
2. Böhringer, N.; Kramer, J. C.; de la Mora, E.; Padva, L.; Wuisan, Z. G.; Liu, Y.; Kurz, M.; Marner, M.; Nguyen, H.; Amara, P.; Yokoyama, K.; Nicolet, Y.; Mettal, U.; Schäberle, T. F. Genome- and metabolome-guided discovery of marine BamA inhibitors revealed a dedicated darobactin halogenase. *Cell Chem. Biol.* **2023**, *30*, 943–952.
3. Freeman, M. F.; Gurgui, C.; Helf, M. J.; Morinaka, B. I.; Uria, A. R.; Oldham, N. J.; Sahl, H. G.; Matsunaga, S.; Piel, J. Metagenome mining reveals polytheonamides as posttranslationally modified ribosomal peptides. *Science* **2012**, *338*, 387–390.
4. Huo, L.; Ökesli, A.; Zhao, M.; van der Donk, W. A. Insights into the Biosynthesis of Duramycin. *Appl. Environ. Microbiol.* **2017**, *83*, e02698-16.
5. Zhang, C.; Seyedsayamdost, M. R. CanE, an Iron/2-Oxoglutarate-Dependent Lasso Peptide Hydroxylase from *Streptomyces canus*. *ACS Chem. Biol.* **2020**, *15*, 890–894.
6. Sugiyama, R.; Suarez, A. F. L.; Morishita, Y.; Nguyen, T. Q. N.; Tooh, Y. W.; Roslan, M. N. H. B.; Lo Choy, J.; Su, Q.; Goh, W. Y.; Gunawan, G. A.; Wong, F. T.; Morinaka, B. I. The Biosynthetic Landscape of Triceptides Reveals Radical SAM Enzymes That Catalyze Cyclophane Formation on Tyr- and His-Containing Motifs. *J. Am. Chem. Soc.* **2022**, *144*, 11580-11593
7. Kim, H. W.; Kang, S.; Kim, S.; Lee, H.; Hur, Y.; Song, W. J.; Oh, D. C.; Kim, S. Discovery of a Two-Step Enzyme Cascade Converting Aspartate to Aminomalonate in Peptide Natural Product Biosynthesis. *J. Am. Chem. Soc.* **2025**, *147*, 20909–20918.
8. Morishita, Y.; Ma, S.; De La Mora, E.; Li, H.; Chen, H.; Ji, X.; Usclat, A.; Amara, P.; Sugiyama, R.; Tooh, Y. W.; Gunawan, G.; Pérard, J.; Nicolet, Y.; Zhang, Q.; Morinaka, B. I. Fused radical SAM and αKG-HExxH domain proteins contain a distinct structural fold and catalyse cyclophane formation and β-hydroxylation. *Nat. Chem.* **2024**, *16*, 1882–1893.
9. Ouyang, Y.; Yu, Y.; Zhu, L.; Nguyen, D. T; van der Donk, W. A. Oxidative peptide backbone cleavage by a HexxH enzyme during RiPP biosynthesis. *J. Am. Chem. Soc*. **2026**, *148*, 3551-3561.
10. Shi, J.; Zhang, Y.; Ren, W. Q.; Shi, Y.; Wei, Y. Y.; Zhang, B.; Jiao, R. H.; Ge, H. M. Biosynthesis of collinodin unveils iterative oxidative and prenylation modifications. *ACS Catal*. **2025**, *15*, 6628-6639.
11. Madeira, F.; Madhusoodanan, N.; Lee, J.; Eusebi, A.; Niewielska, A.; Tivey, A. R. N.; Lopez, R.; Butcher, S. The EMBL-EBI Job Dispatcher sequence analysis tools framework in 2024. *Nucleic Acids Res.* **2024**, *52*, W521–W525.
12. Holm, L.; Laiho, A.; Törönen, P.; Salgado, M. DALI shines a light on remote homologs: One hundred discoveries. *Protein Sci*. **2023**, *32*, e4519.
13. Abramson, J.; Adler, J.; Dunger, J.; Evans, R.; Green, T.; Pritzel, A.; Ronneberger, O.; Willmore, L.; Ballard, A. J.; Bambrick, J.; Bodenstein, S. W.; Evans, D. A.; Hung, C. C.; O'Neill, M.; Reiman, D.; Tunyasuvunakool, K.; Wu, Z.; Žemgulytė, A.; Arvaniti, E.; Beattie, C.; Bertolli, O.; Bridgland, A.; Cherepanov, A.; Congreve, M.; Cowen-Rivers, A. I.; Cowie, A.; Figurnov, M.; Fuchs, F. B.; Gladman, H.; Jain, R.; Khan, Y. A.; Low, C. M. R.; Perlin, K.; Potapenko, A.; Savy, P.; Singh, S.; Stecula, A.; Thillaisundaram, A.; Tong, C.; Yakneen, S.; Zhong, E. D.; Zielinski, M.; Žídek, A.; Bapst, V.; Kohli, P.; Jaderberg, M.; Hassabis, D.; Jumper, J. M. Accurate structure prediction of biomolecular interactions with AlphaFold 3. *Nature* **2024**, *630*, 493-500.
14. Corpet, F. Multiple sequence alignment with hierarchical clustering. *Nucleic Acids Res*. **1988**, *16*, 10881–10890.
15. Schnell, N.; Entian, K. D.; Schneider, U.; Götz, F.; Zähner, H.; Kellner, R.; Jung, G. Prepeptide sequence of epidermin, a ribosomally synthesized antibiotic with four sulphide-rings. *Nature* **1988**, *333*, 276–278.
16. Sikandar, A.; Lopatniuk, M.; Luzhetskyy, A.; Müller, R.; Koehnke, J. Total In Vitro Biosynthesis of the Thioamitide Thioholgamide and Investigation of the Pathway. *J. Am. Chem. Soc*. **2022**, *144*, 5136–5144.
17. Wiebach, V.; Mainz, A.; Siegert, M. J.; Jungmann, N. A.; Lesquame, G.; Tirat, S.; Dreux-Zigha, A.; Aszodi, J.; Le Beller, D.; Süssmuth, R. D. The anti-staphylococcal lipolanthines are

ribosomally synthesized lipopeptides. *Nat. Chem. Biol*. **2018**, *14*, 652–654.
18. Wang, S.; Lin, S.; Fang, Q.; Gyampoh, R.; Lu, Z.; Gao, Y.; Clarke, D. J.; Wu, K.; Trembleau, L.; Yu, Y.; Kyeremeh, K.; Milne, B. F.; Tabudravu, J.; Deng, H. A ribosomally synthesised and post-translationally modified peptide containing a β-enamino acid and a macrocyclic motif. *Nat. Commun.* **2022**, *13*, 5044.
19. Ishikawa, N.; Tanaka, H.; Koyama, F.; Noguchi, H.; Wang, C. C.; Hotta, K.; Watanabe, K. Non-heme dioxygenase catalyzes atypical oxidations of 6,7-bicyclic systems to form the 6,6-quinolone core of viridicatin-type fungal alkaloids. *Angew. Chem. Int. Ed*. **2014**, *53*, 12880–12884.
20. Meng, S.; Han, W.; Zhao, J.; Jian, X. H.; Pan, H. X.; Tang, G. L. A Six-Oxidase Cascade for Tandem C-H Bond Activation Revealed by Reconstitution of Bicyclomycin Biosynthesis. *Angew. Chem. Int. Ed*. **2018**, *57*, 719–723.
21. Vynne, N. G.; Mansson, M.; Gram, L. Gene sequence based clustering assists in dereplication of *Pseudoalteromonas luteoviolacea* strains with identical inhibitory activity and antibiotic production. *Mar. Drugs* **2012**, *10*, 1729–1740.